Supporting Information For:

Molecular Dynamics Study of *Helicobacter pylori* Urease

Mona S. Minkara, Melek N. Ucisik, Michael N. Weaver and Kenneth M. Merz, Jr.*

Table of Contents

Expanded Wide-Open State Analysis

HISα320 is a critical residue proposed to play an integral role in the urea hydrolysis mechanism for *K. aerogenes* and *B. pasteurii* ureases[1,2] and displacement of this residue is thought to be essential in reaching the wide-open flap state, allowing urea access to the active site. The corresponding residue in *H. pylori* urease is HISα322. Figure S1 shows that in the flap that achieves the wide-open state, the HISα322/GLYα47 separation starts around 8 Ångstroms, close to the value observed in the closed flap state, but as the simulation proceeds, the separation of these residues reaches a maximum of 20 Ångstroms, with distinct separation from the semi-open state occurring approximately 100ns into the simulation. The trajectory clearly reveals a marked displacement of the histidine in achieving the wide-open state both in comparison to the closed and semi-open states. In the closed state this separation is nearly constant at approximately 7 Ångstroms while in the semi-open state the separation is roughly 10 Ångstroms.

The separation between GLUα330/ALAβ173 is observed to fluctuate in concert with the ILEα328/ALAβ170 distances, with the former separation reaching a maximum of ~30 Ångstroms in the wide-open state (Figure S2). This separation is also observed to narrow over the last quarter of the MD run and begins its decline slightly earlier than the ILEα328/ALAβ170 separation. In the wide-open flap state all the identified residue pairs have separations that vary in phase with one another, which is in contrast to the semi-open flap state that has been reported previously in the literature.[HA] The semi-open flap state is observed in the other 10 flaps and in these cases the ILEα328/ALAβ170 and GLUα330/ALAβ173 separations fluctuate in a synchronized manner, while the HISα322/GLYα47 separation fluctuates out of phase with respect to

the former two separations. This behavior is expected, since ILEα328 and GLUα330 are only 2 amino acids apart and are more likely to move in a concerted fashion. The plots containing the residue separations for remaining flaps are presented elsewhere in the Supporting Information (Figures S11-S19). It is further pointed out that each of the distances discussed is shorter in the X-ray structure, 12.87 Ångsttroms for ILEα328/ALAβ170, 4.91 Ångstroms for GLUα330/ALAβ173 and 3.85 Ångstroms for HISα322/GLYα47.

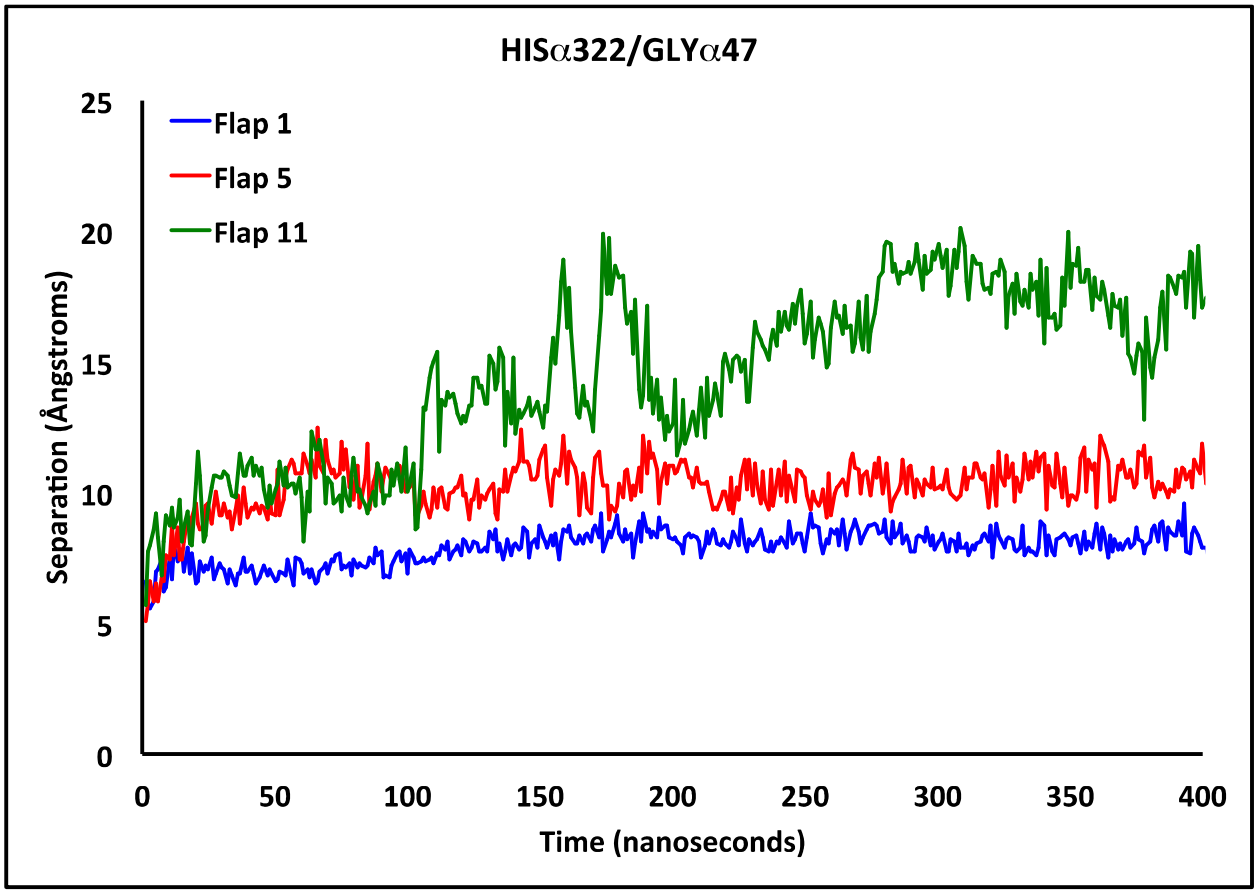

Figure S1: Separation between residues HISα332 and GLYα47 over time for flaps representing the closed (blue), semi-open (red) and wide-open (green) flap states.

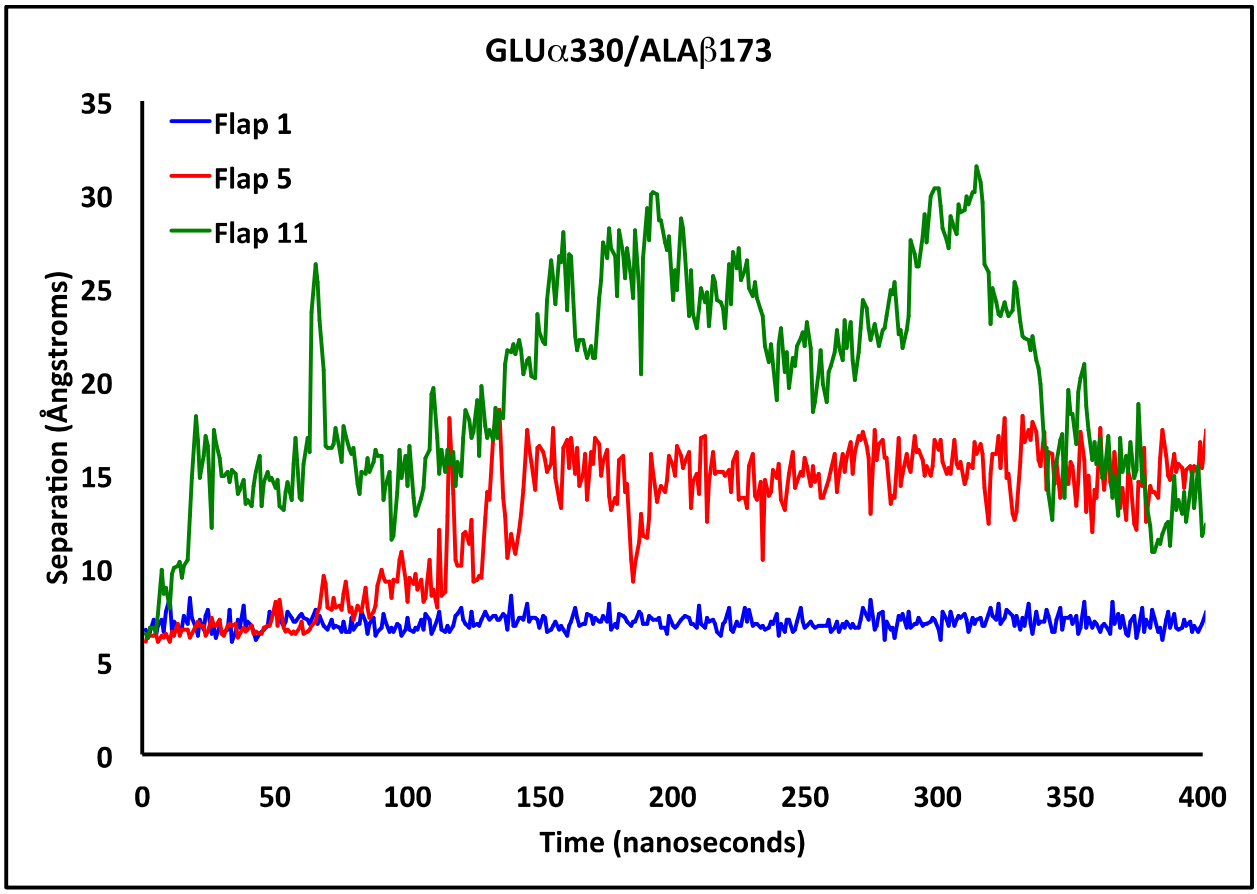

Figure S2: Separation between residues GLUα330 and ALAβ173 over time for flaps representing the closed (blue), semi-open (red) and wide-open (green) flap states.

Ni-HIS Distances

One of the mechanisms proposed in the literature for the hydrolysis of urea by *K. aerogenes* urease involves HISα320 on the flap interacting with the bridging hydroxide.[1] This hydrogen bonding interaction with the histidine is thought to be critical for urea hydrolysis and this residue corresponds to HISα322 in *H. pylori*. The hypothesis is that the wide-open flap state will have this histidine removed far enough from the nickel centers to permit a molecule of urea to enter the active site and interact with the pentacoordinate Ni^{2+} ion. In order to analyze this separation over the course of the MD

simulation, the distance between the HISα322 αC and the two Ni^{2+} ions for each frame were extracted and plotted (Figure S3, Figures S16-S20). As expected, the closed flap (flap1) had very small ranges in which the separations between both Ni^{2+} ions and the histidine were observed to vary between 9 and 11 Ångstroms. For the wide-open flap (flap11) the separations range from 9 to 27 Ångstroms, a 9-fold increase in the ranges spanned by the flap1 distances. In the other 10 cases we observed flaps that are beginning to show wide-open flap state character. This is typically manifested as the unraveling of one, but not both, of the α-helices that make up the flap. For example flaps 2, 5 and 8 have ranges from 9 to 17 Ångstroms, which clearly reveal that the HIS residue is far away enough for a urea molecule to enter the active site. As for the other flaps, they have ranges of separation spanning from 9 to 14 Ångstroms.

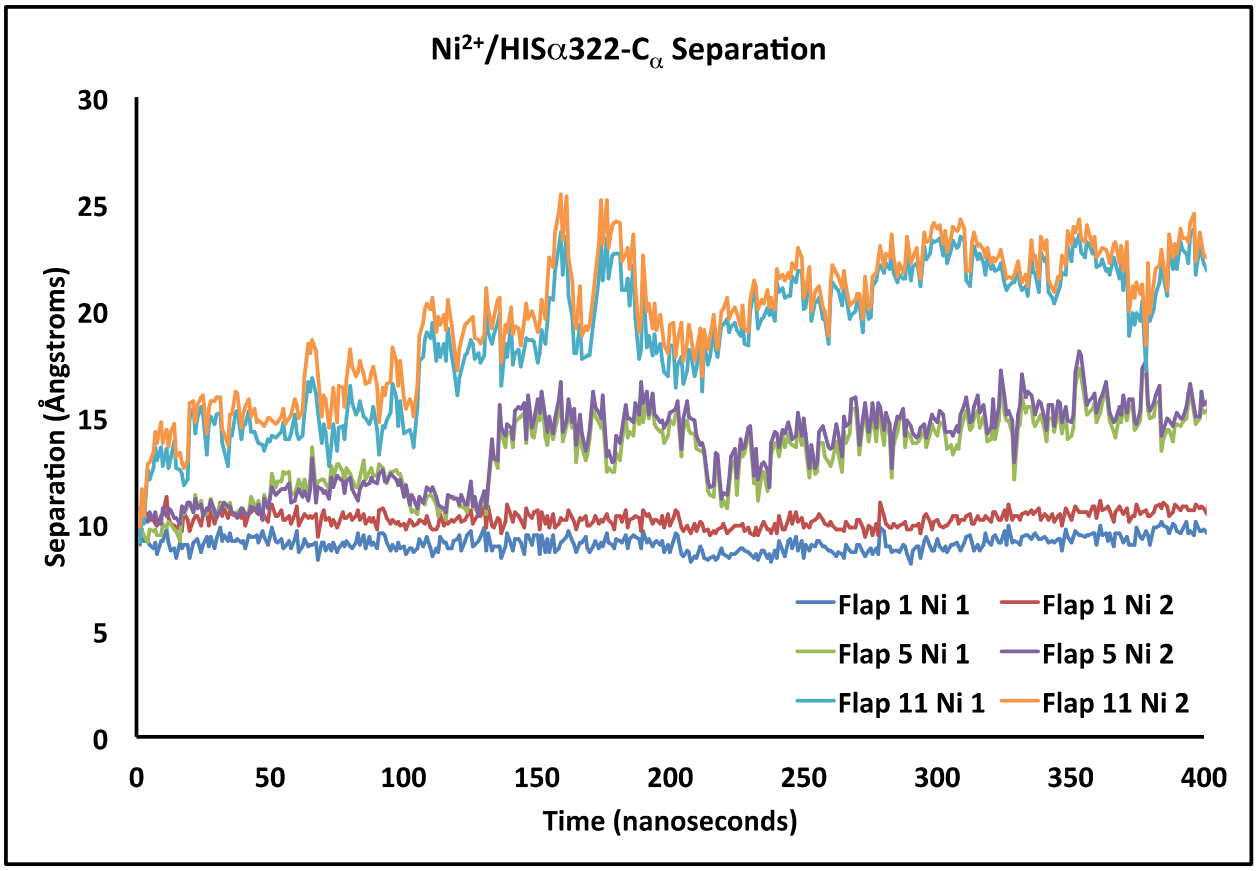

Figure S3: Ni^{2+}/HISα322-αC distance fluctuations for the various flaps.

In order to further probe the importance of this key HIS residue, we extracted and plotted the distances between the HISα322-εN to both Ni^{2+} ions for each flap. All but 2 flaps exhibit regions where the εN/Ni^{2+} distance dramatically increases. Representative separations over the course of the MD simulation are presented in Figure S4 for the closed, semi-open and wide-open flap states with remaining plots presented in Figures S21-23 (see Supporting Information). In the flap that remains closed throughout the entire simulation, the minimum distance between the HIS322-εN and the pentacoordinate Ni^{2+} is 4.5 Ångstroms. This pentacoordinate nickel is the closest of the nickel ions to the HISα322 εN in nearly all cases. For the first flap, which was observed to remain closed,

the maximum εN/Ni^{2+} separation is 9 Ångstroms. As for the other 10 flaps that exhibit a semi-open flap state there are sharp peaks indicative of large increases in the εN/Ni^{2+} separation and the maximum found in the 10 flaps that exhibit a semi-open flap state is 20 Ångstroms. As for the wide-open flap state the distance gradually increases reaching a maximum of 31 Ångstroms without a clear sharp peak as exhibited by the other flaps. In the open flap sate the minimum distance is generally around 5 Ångstroms. The rapid increases in the εN/Ni^{2+} separation indicate that the HISα322 imidazole ring undergoes a 180° rotation at a particular point in time resulting in a significant increase in the observed distance between the atoms. Also of note is a region from 50-100 nanoseconds in flap 5 where the εN/Ni^{2+} separations invert, and Ni2 is closer to the εN than Ni1. This is the only flap where this inversion is observed and corresponds to an instance where the imidazole ring rotates 90°.

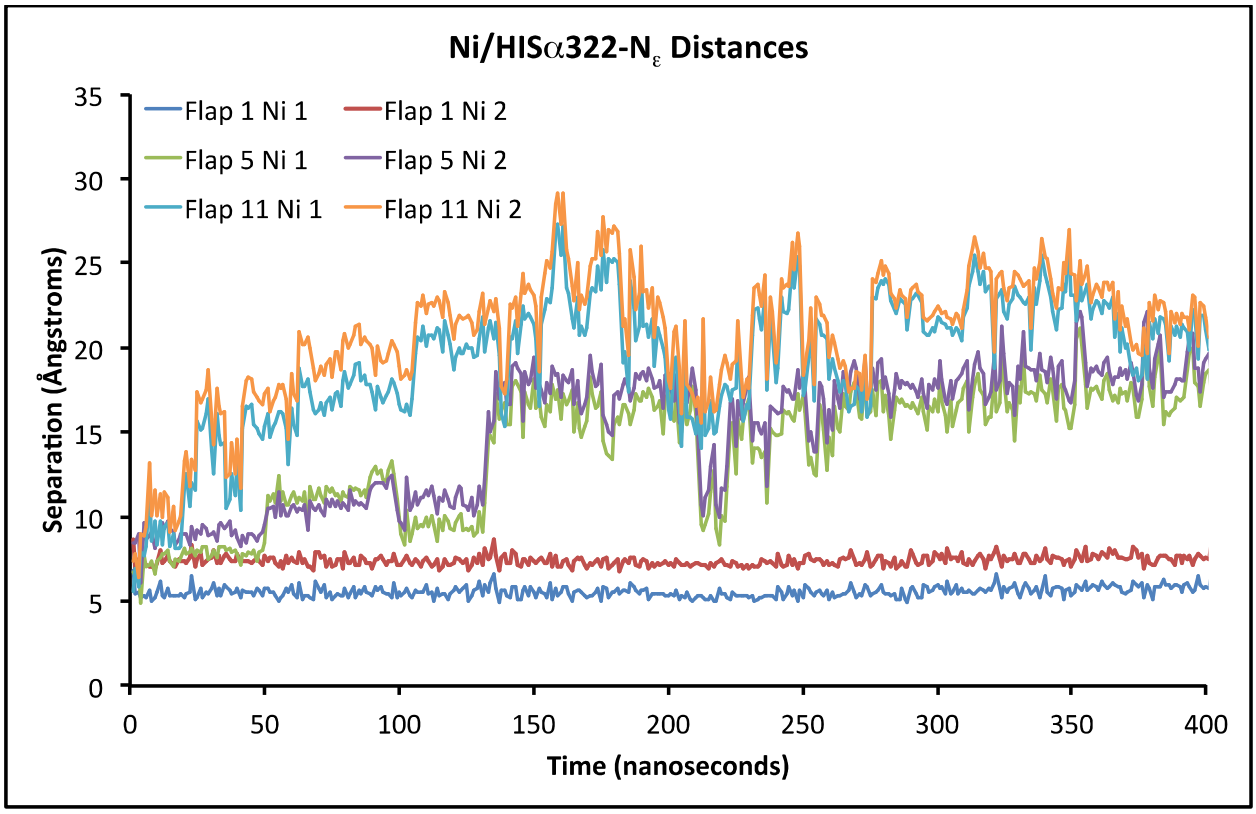

Figure S4: Separation between both active site Ni^{2+} ions and the HISα322-εN for the wide-open, closed and a representative semi-open, state.

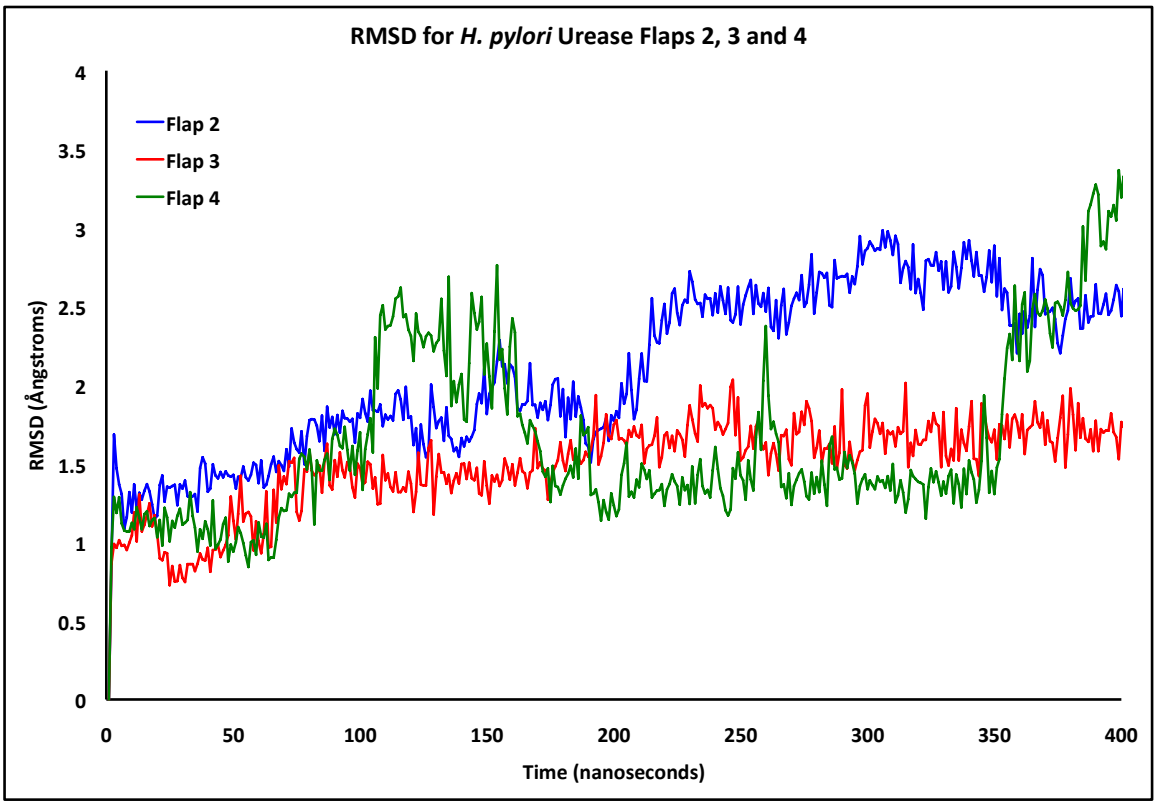

Figure S5: RMSD for *H. pylori* urease flaps 2 (blue), 3 (red) and 4 (green).

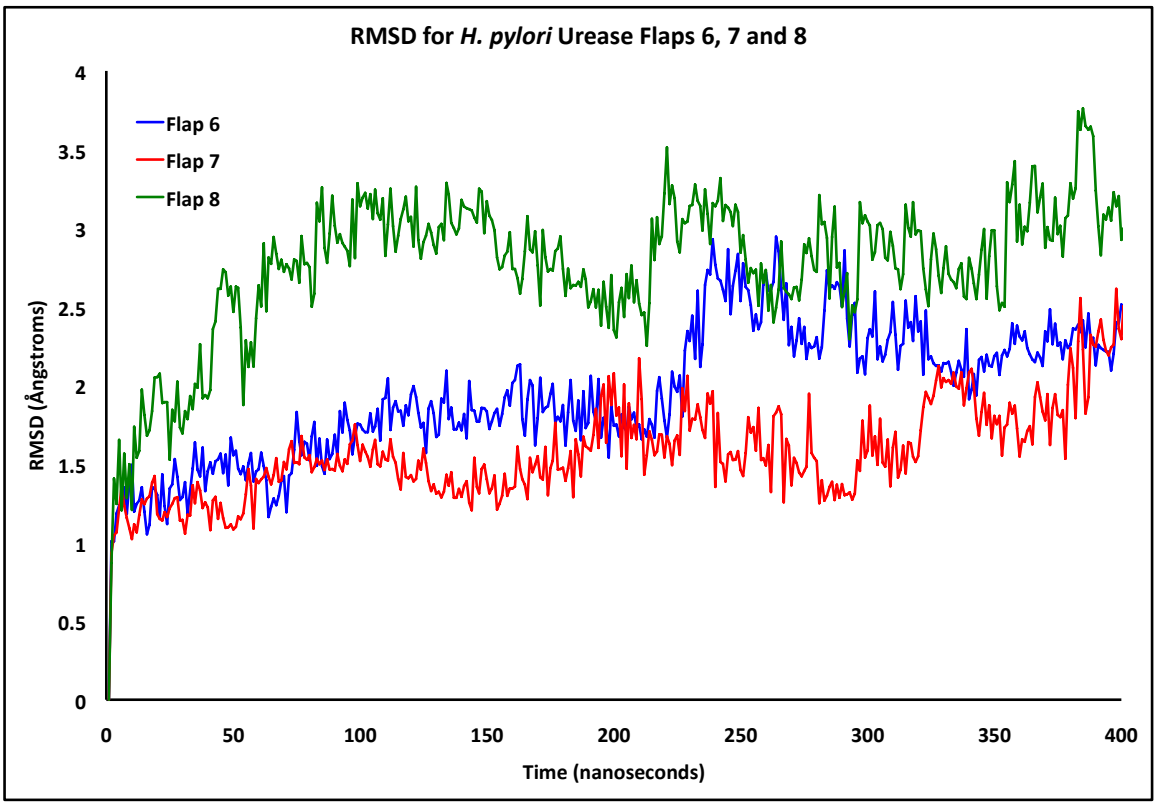

Figure S6: RMSD for *H. pylori* urease flaps 6 (blue), 7 (red) and 8 (green).

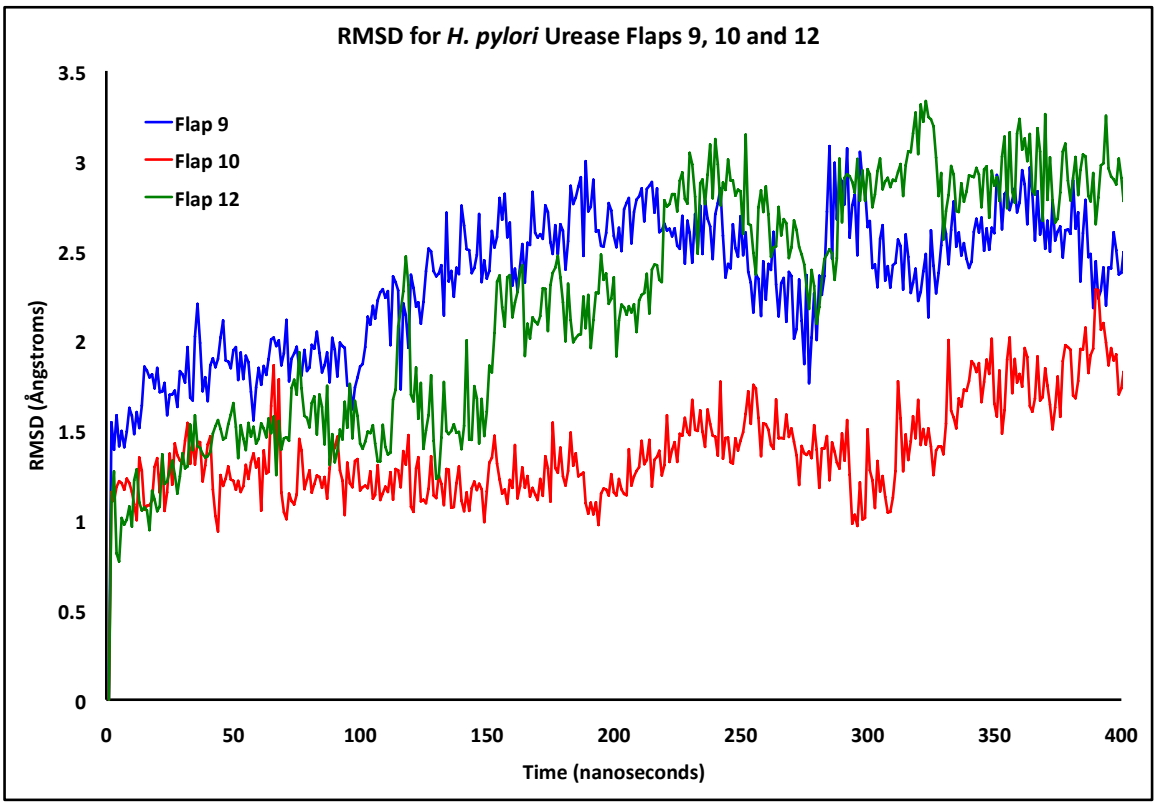

Figure S7: RMSD for *H. pylori* urease flaps 9 (blue), 10 (red) and 12 (green).

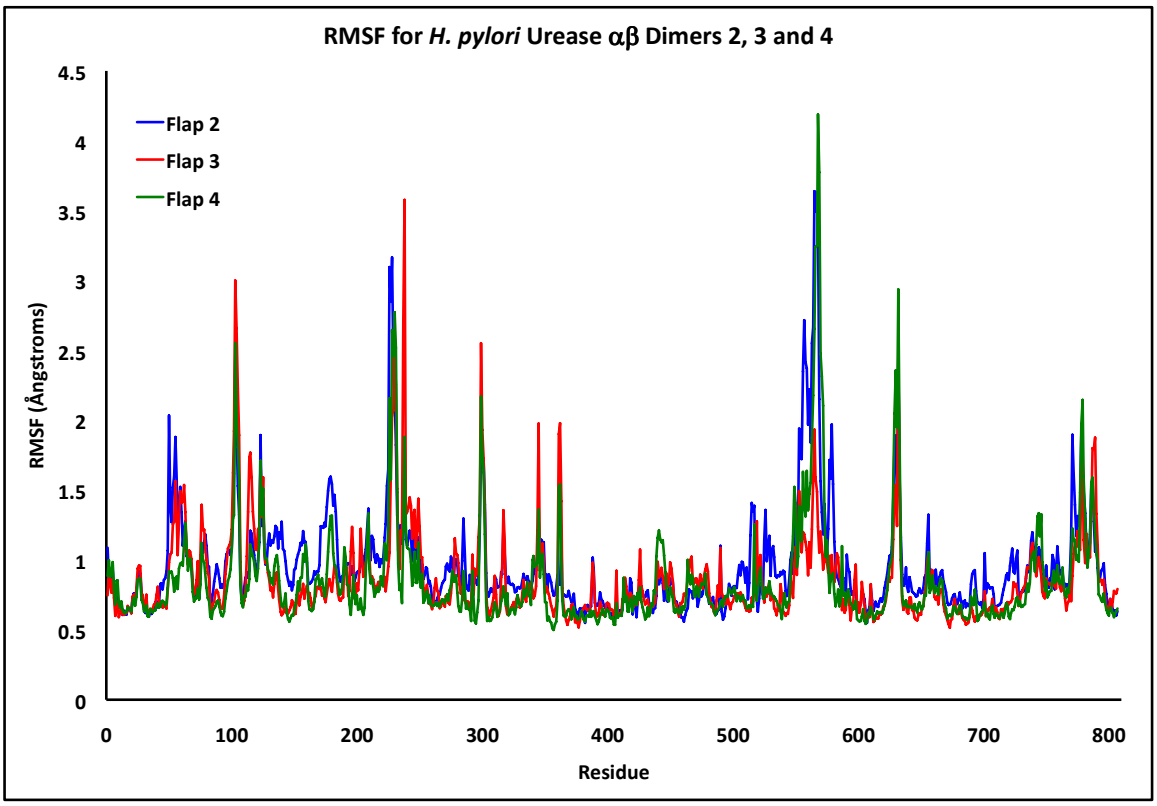

Figure S8: RMSF for *H. pylori* urease dimers 2 (blue), 3 (red) and 4 (green).

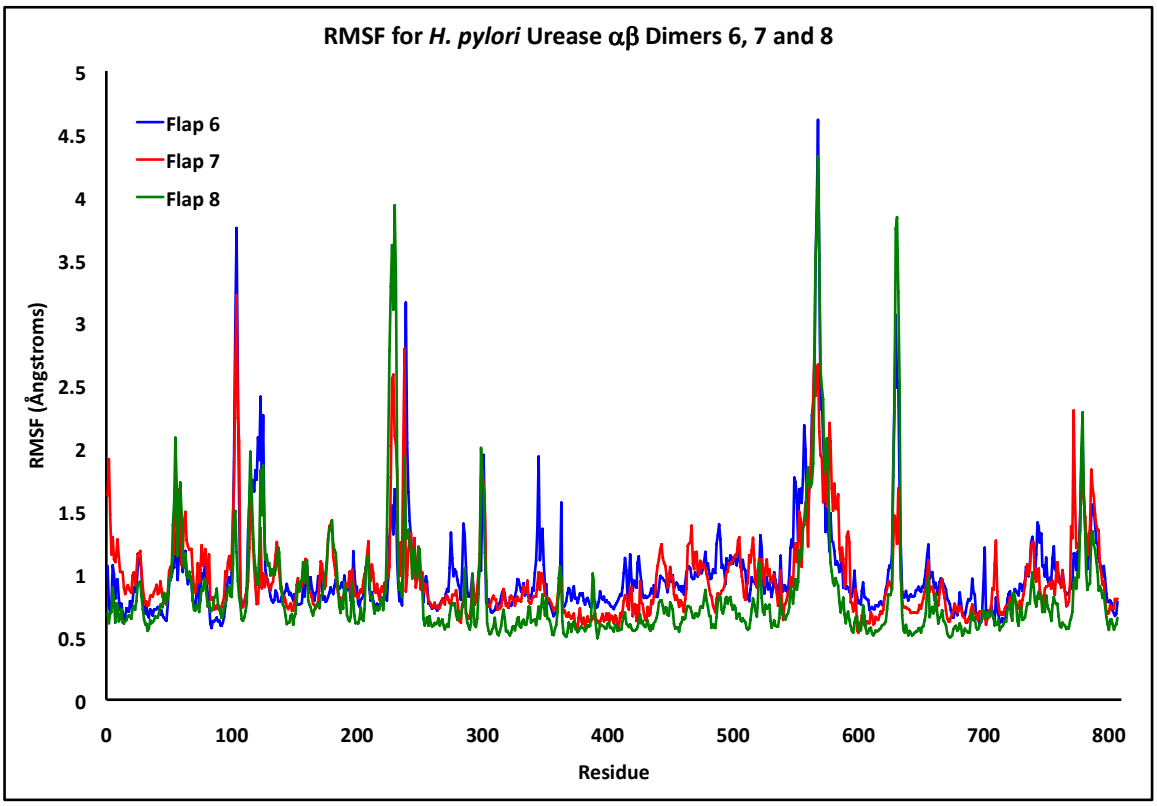

Figure S9: RMSF for *H. pylori* urease dimers 6 (blue), 7 (red) and 8 (green).

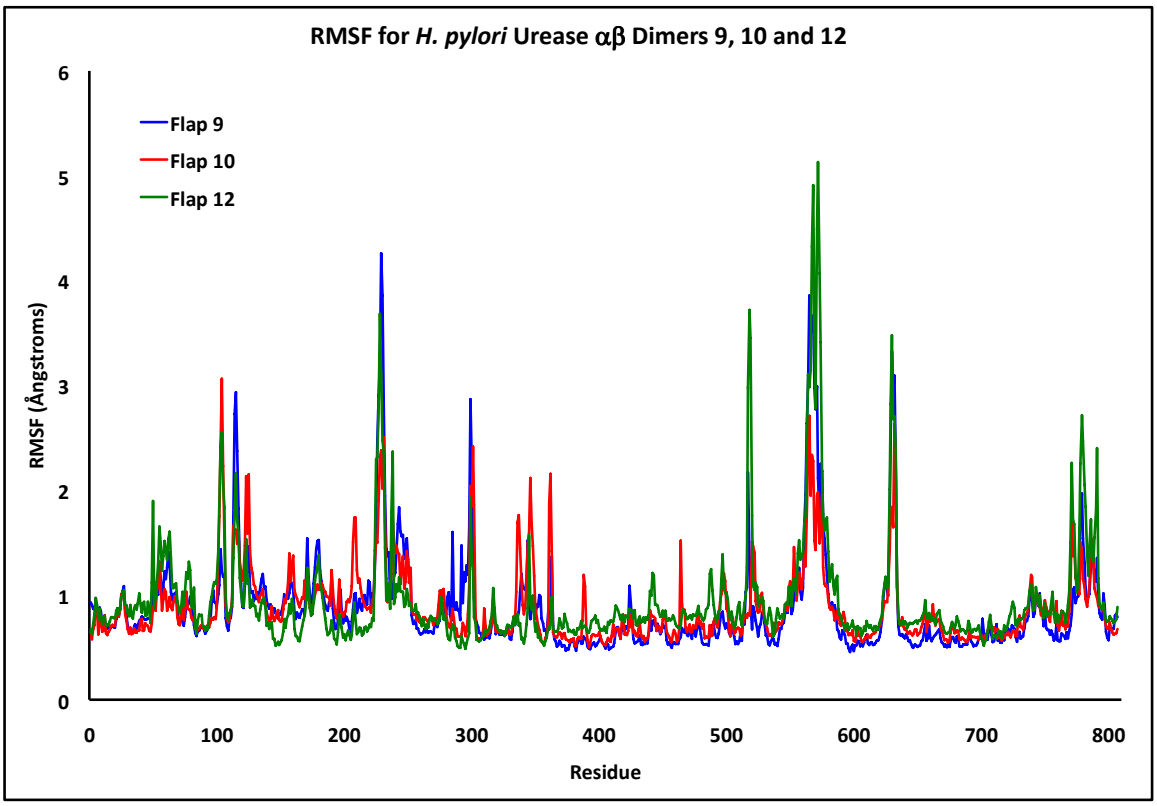

Figure S10: RMSF for *H. pylori* urease dimers 9 (blue), 10 (red) and 12 (green).

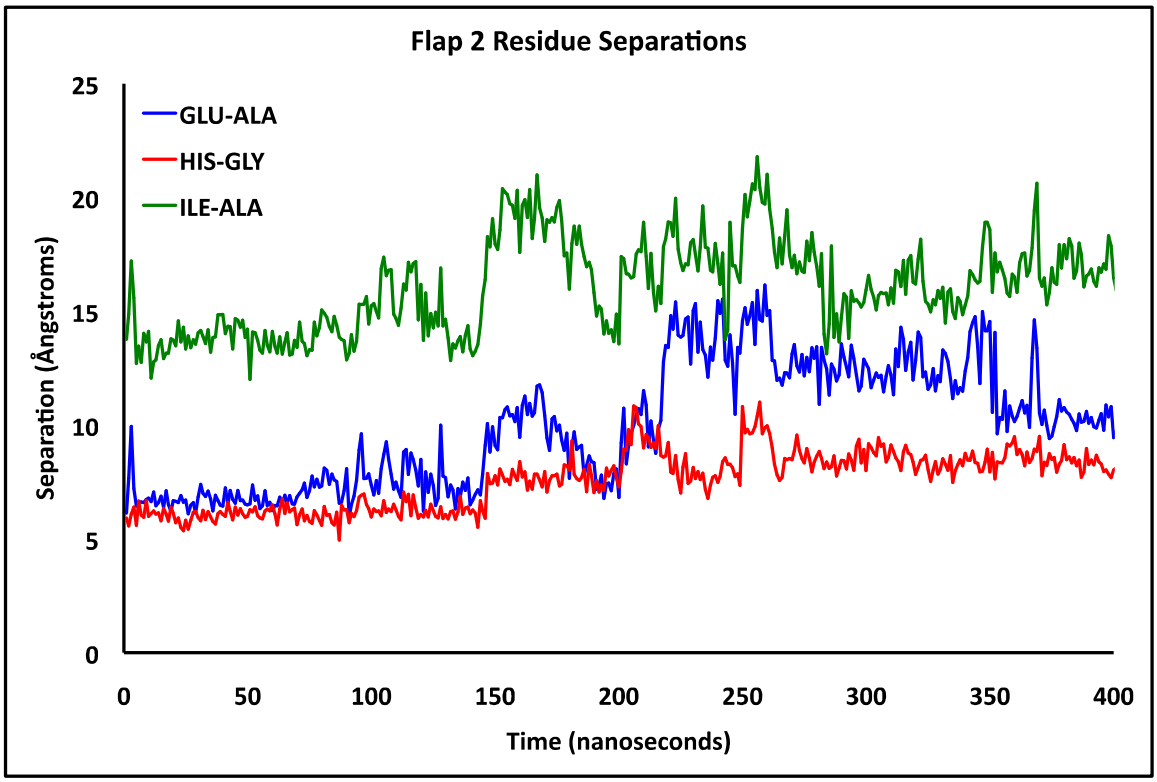

Figure S11: Flap two residue separations between GLUα330/ALAβ173 (blue), HISα322/GLYα47 (red) and ILEα328/ALAβ170 (green) over time.

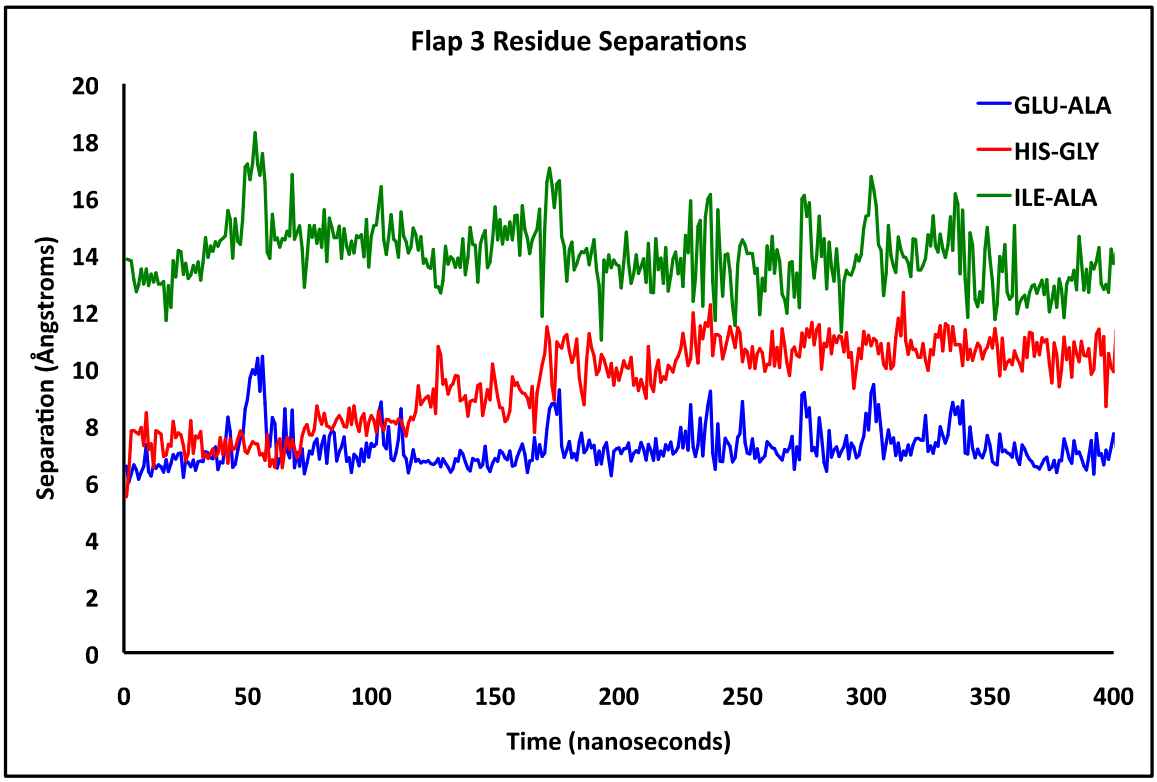

Figure S12: Flap three residue separations between GLUα330/ALAβ173 (blue), HISα322/GLYα47 (red) and ILEα328/ALAβ170 (green) over time.

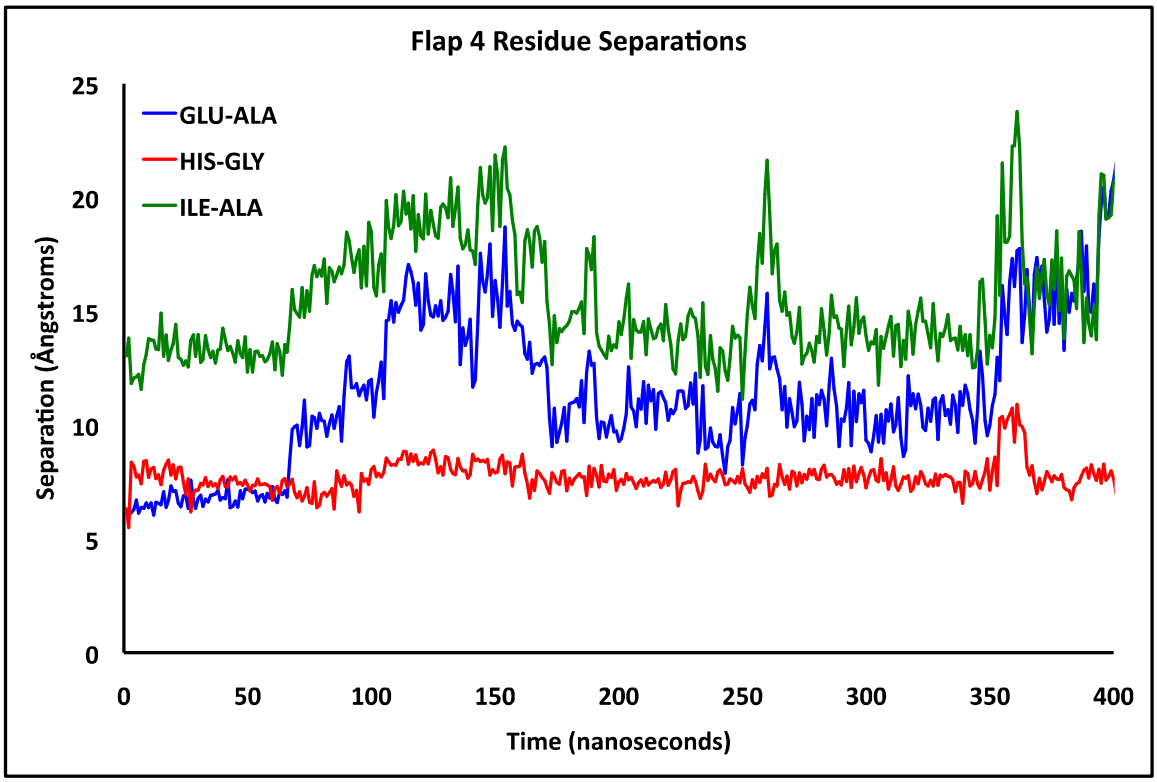

Figure S13: Flap four residue separations between GLUα330/ALAβ173 (blue), HISα322/GLYα47 (red) and ILEα328/ALAβ170 (green) over time.

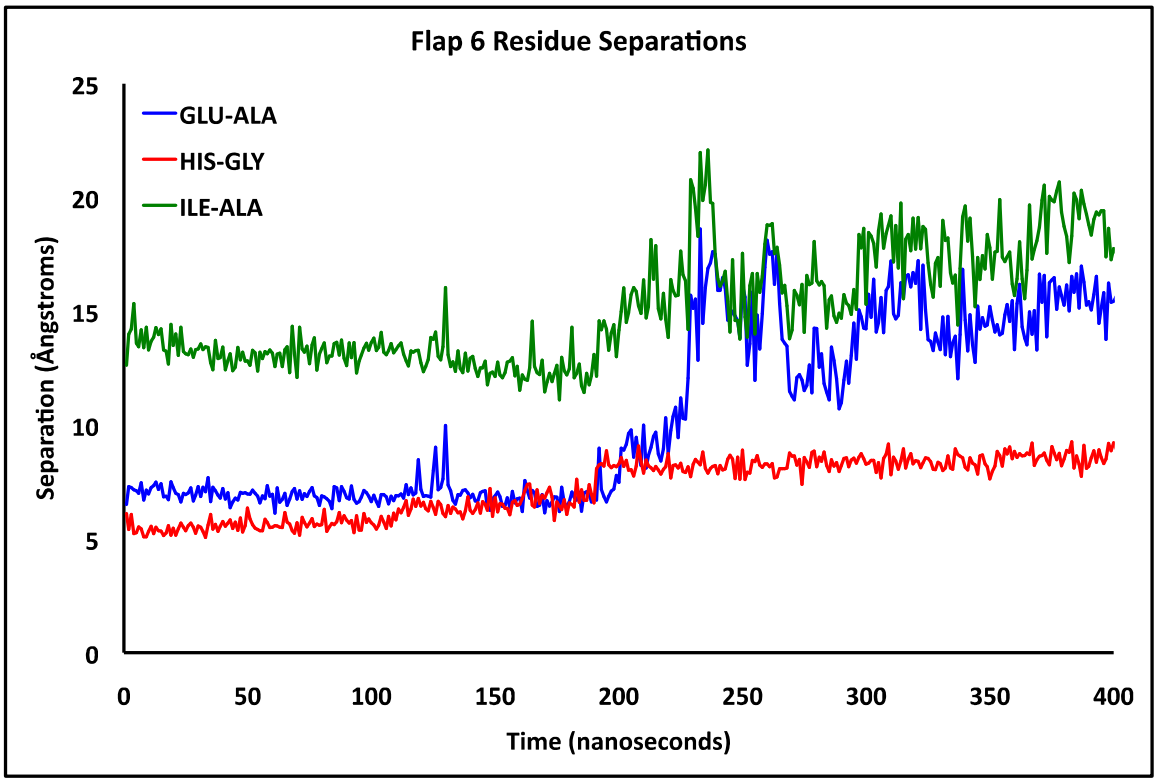

Figure S14: Flap six residue separations between GLUα330/ALAβ173 (blue), HISα322/GLYα47 (red) and ILEα328/ALAβ170 (green) over time.

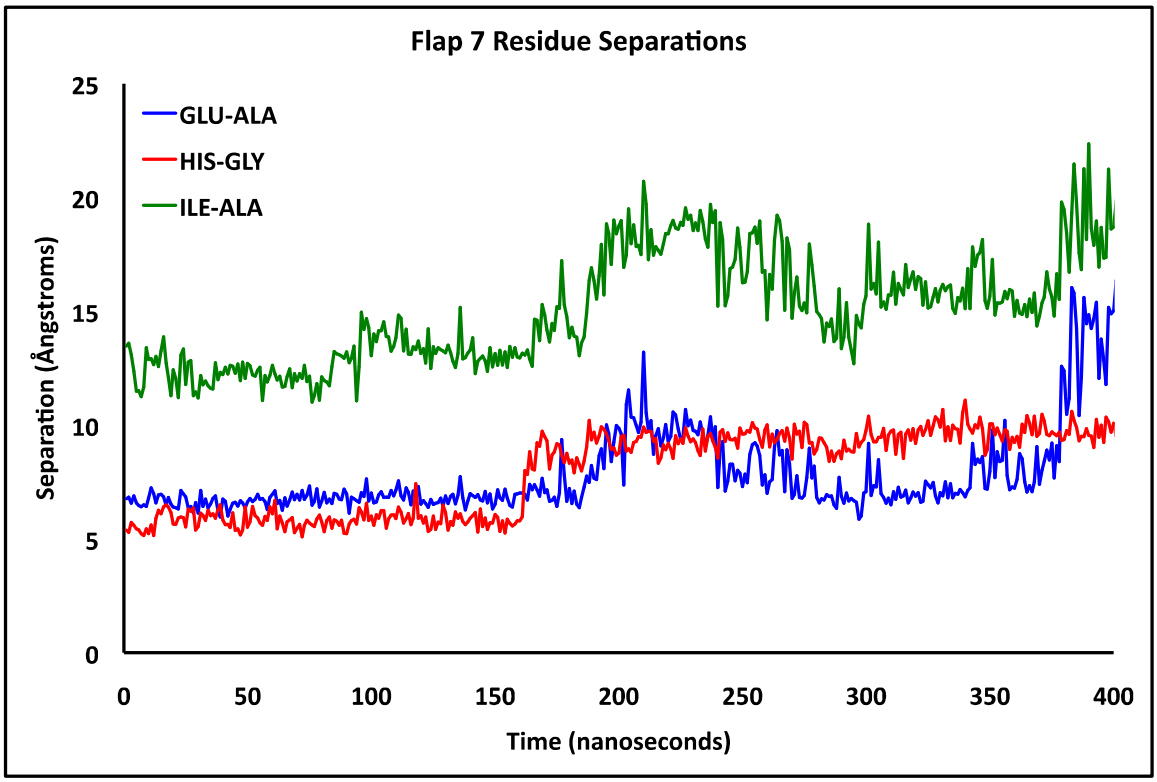

Figure S15: Flap seven residue separations between GLUα330/ALAβ173 (blue), HISα322/GLYα47 (red) and ILEα328/ALAβ170 (green) over time.

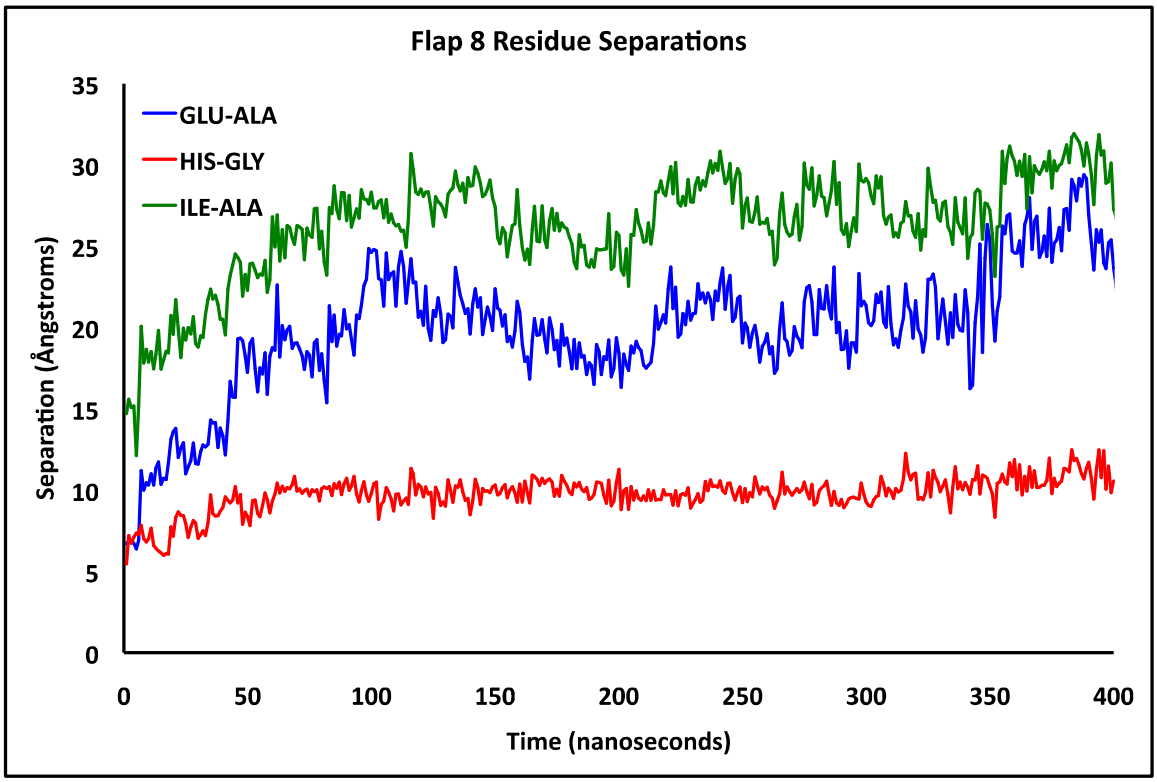

Figure S16: Flap eight residue separations between GLUα330/ALAβ173 (blue), HISα322/GLYα47 (red) and ILEα328/ALAβ170 (green) over time.

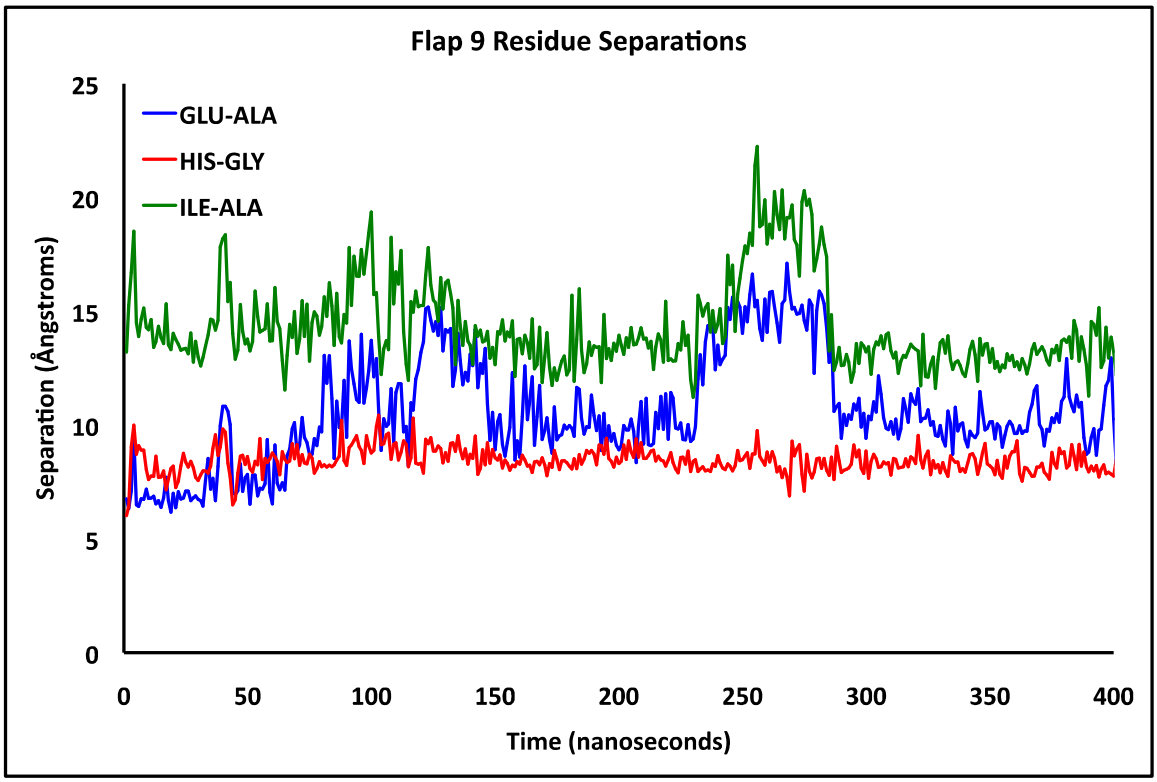

Figure S17: Flap nine residue separations between GLUα330/ALAβ173 (blue), HISα322/GLYα47 (red) and ILEα328/ALAβ170 (green) over time.

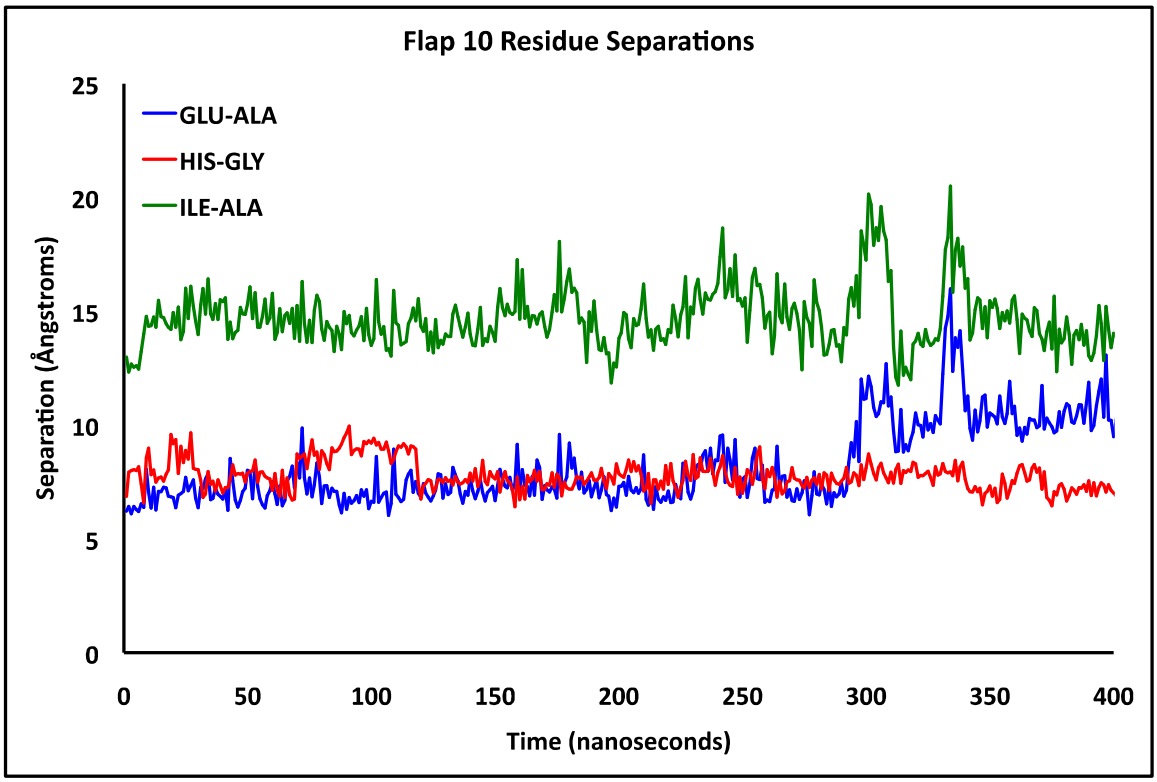

Figure S18: Flap ten residue separations between GLUα330/ALAβ173 (blue), HISα322/GLYα47 (red) and ILEα328/ALAβ170 (green) over time.

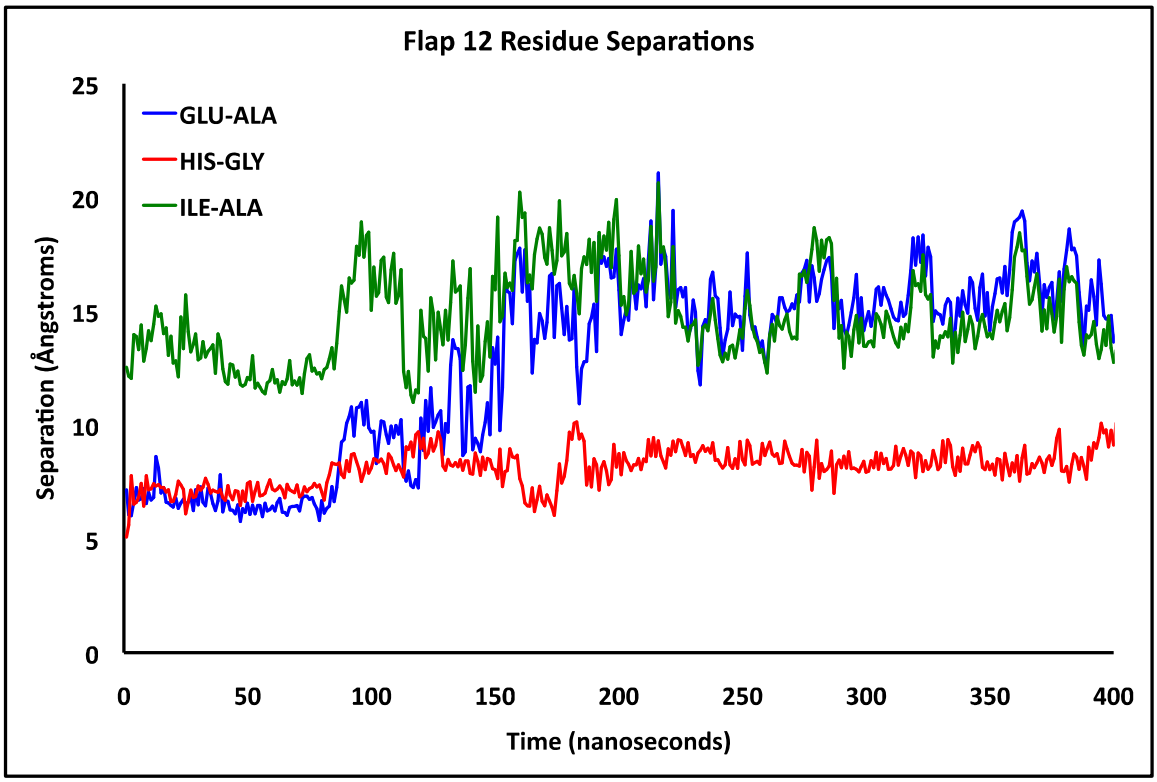

Figure S19: Flap twelve residue separations between GLUα330/ALAβ173 (blue), HISα322/GLYα47 (red) and ILEα328/ALAβ170 (green) over time.

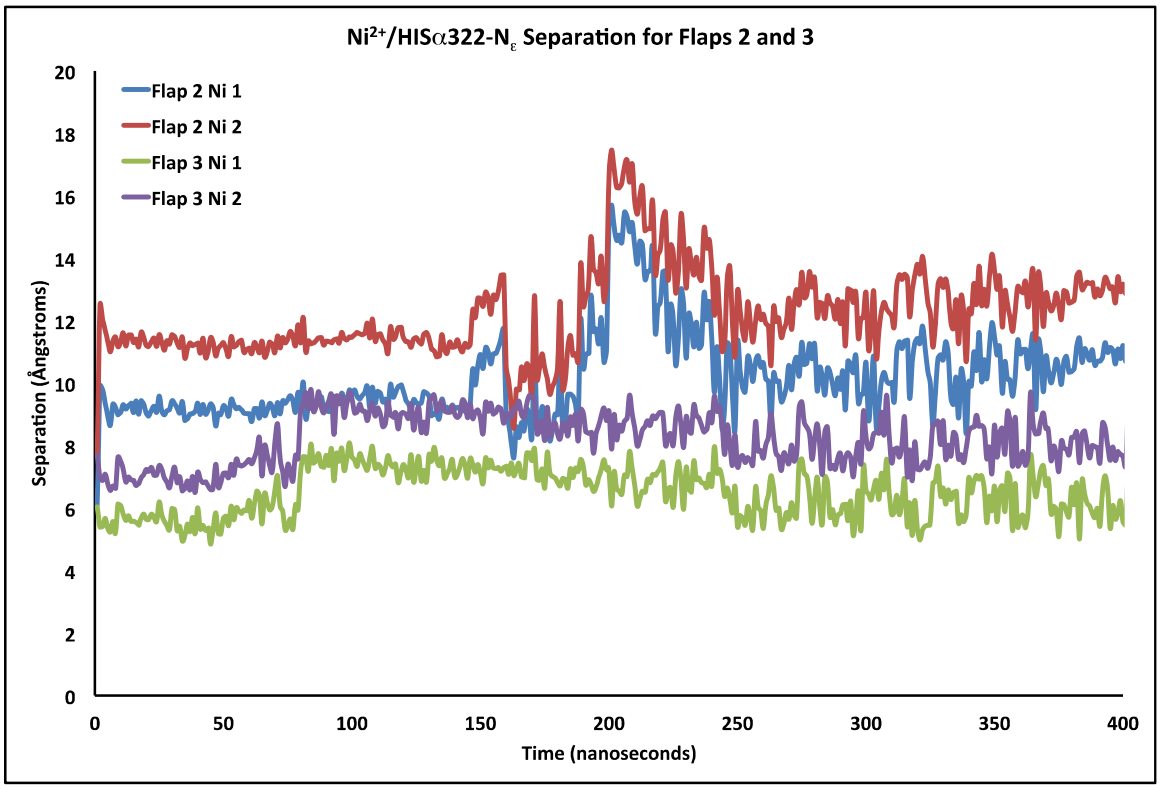

Figure S20: Flap two and three separations between the HISα322-N_ε and each Ni^{2+} ion.

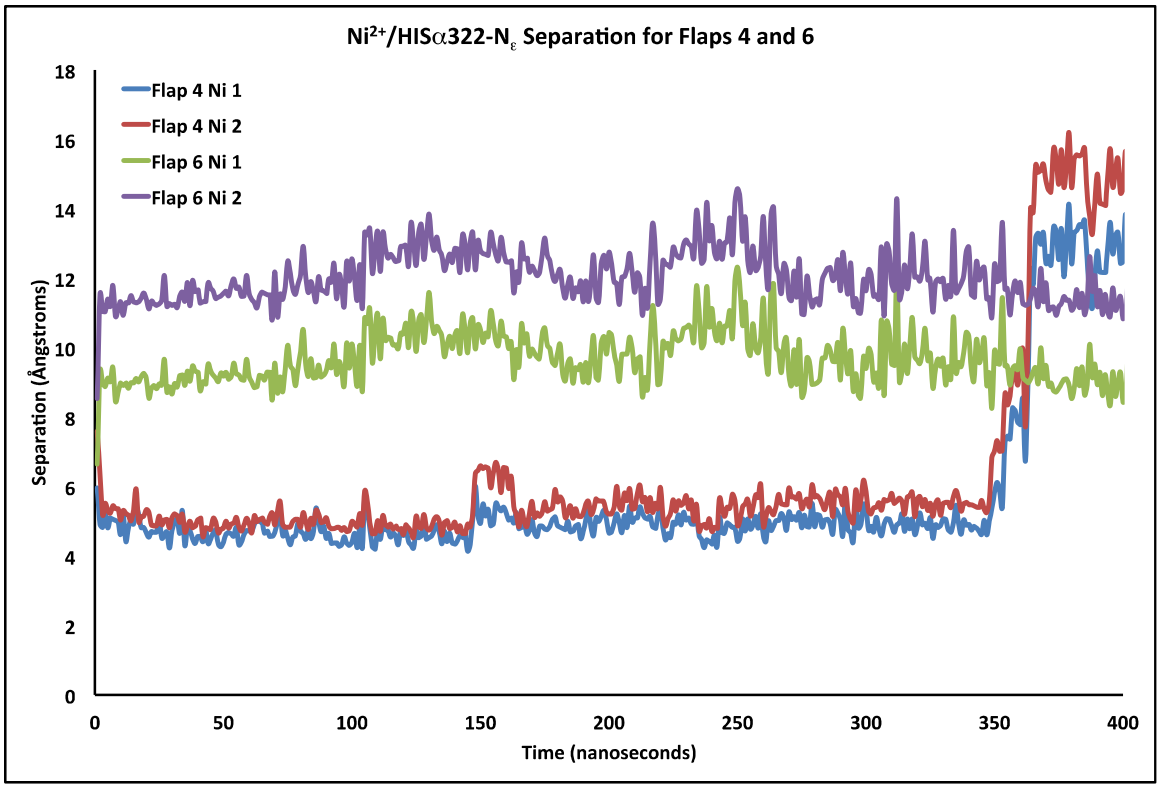

Figure S21: Flap four and six separations between the HISα322-N_ε and each Ni^{2+} ion.

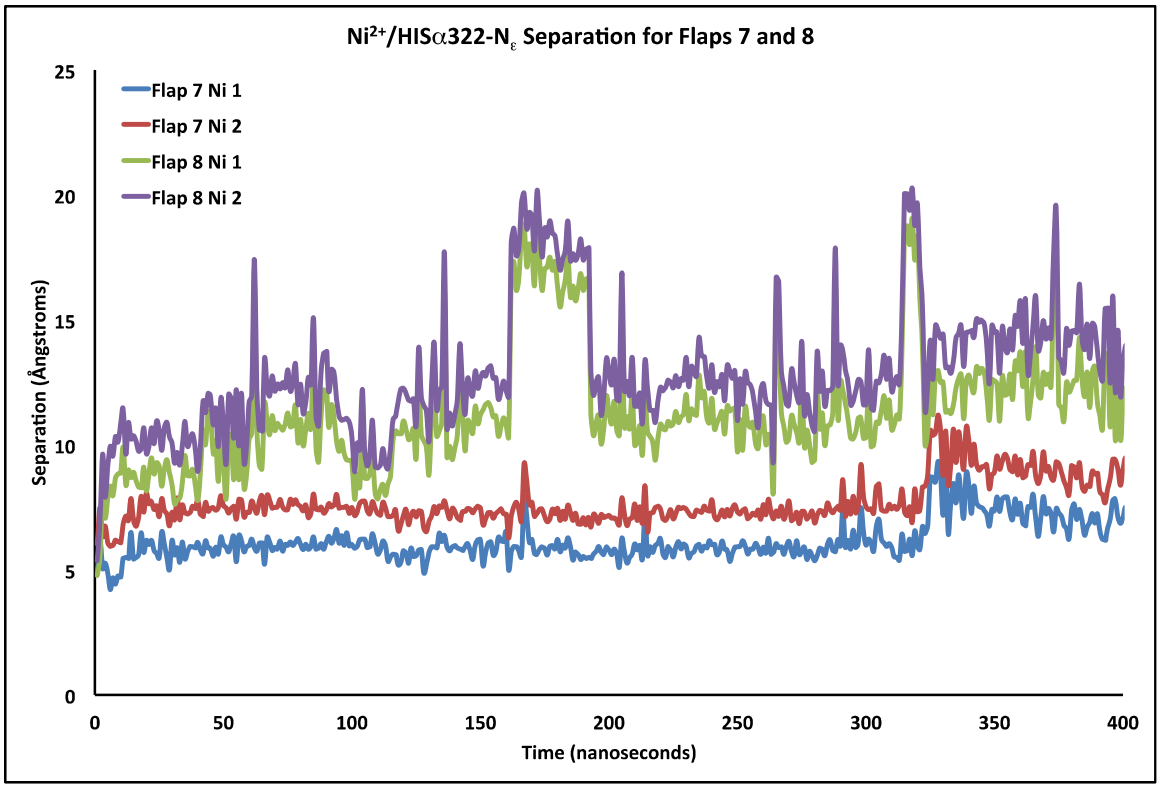

Figure S22: Flap seven and eight separations between the HISα322-N_ε and each Ni^{2+} ion.

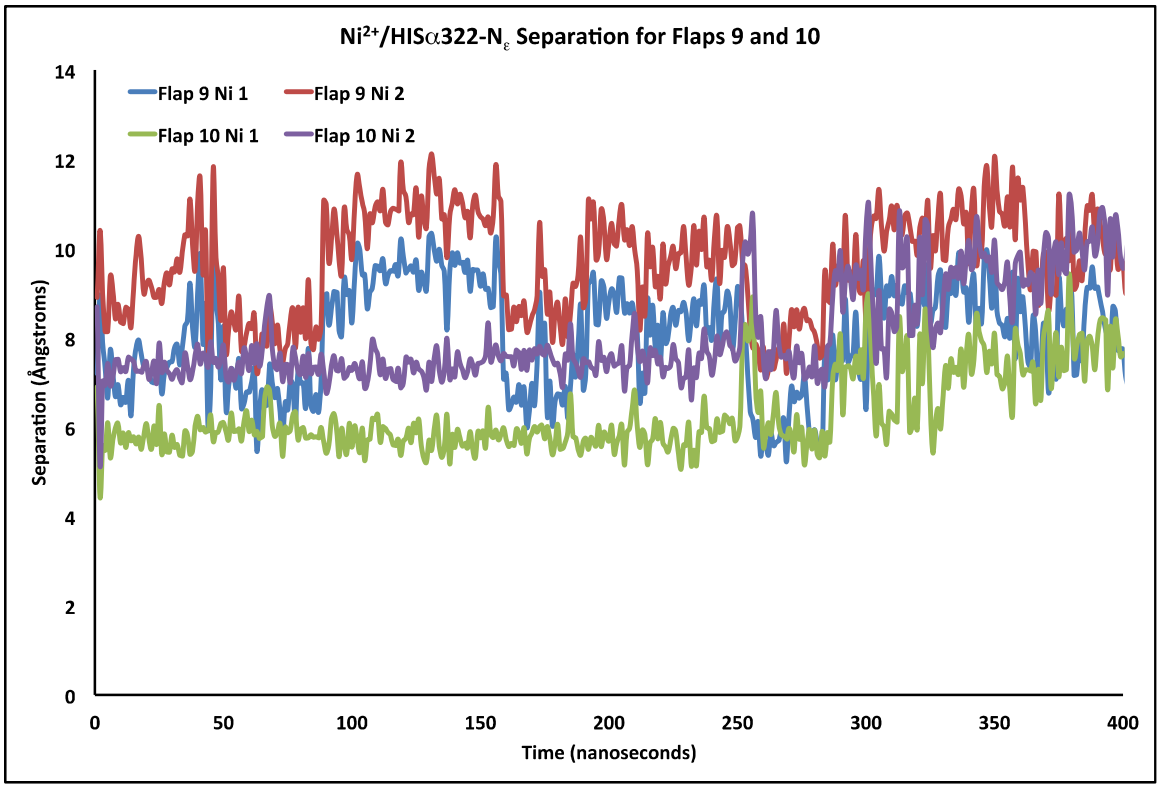

Figure S23: Flap nine and ten separations between the HISα322-N_ε and each Ni^{2+} ion.

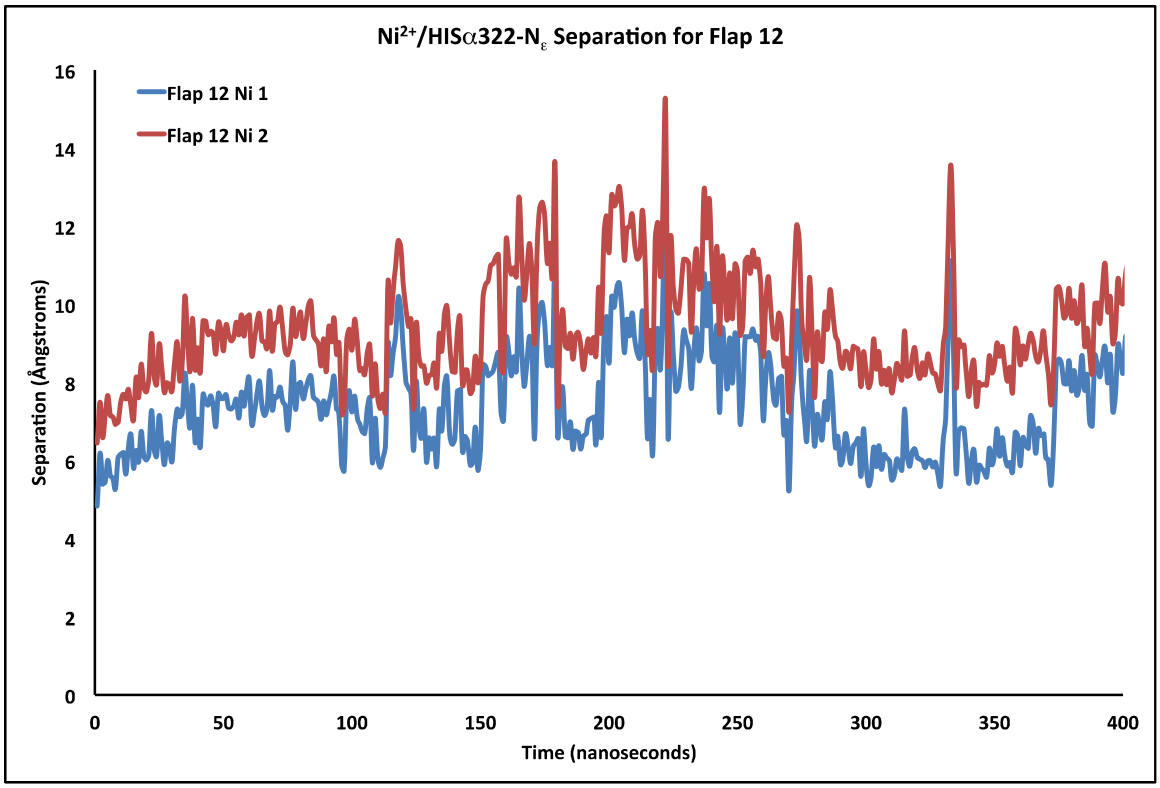

Figure S24: Flap twelve separations between the HISα322-N_ε and each Ni^{2+} ion.

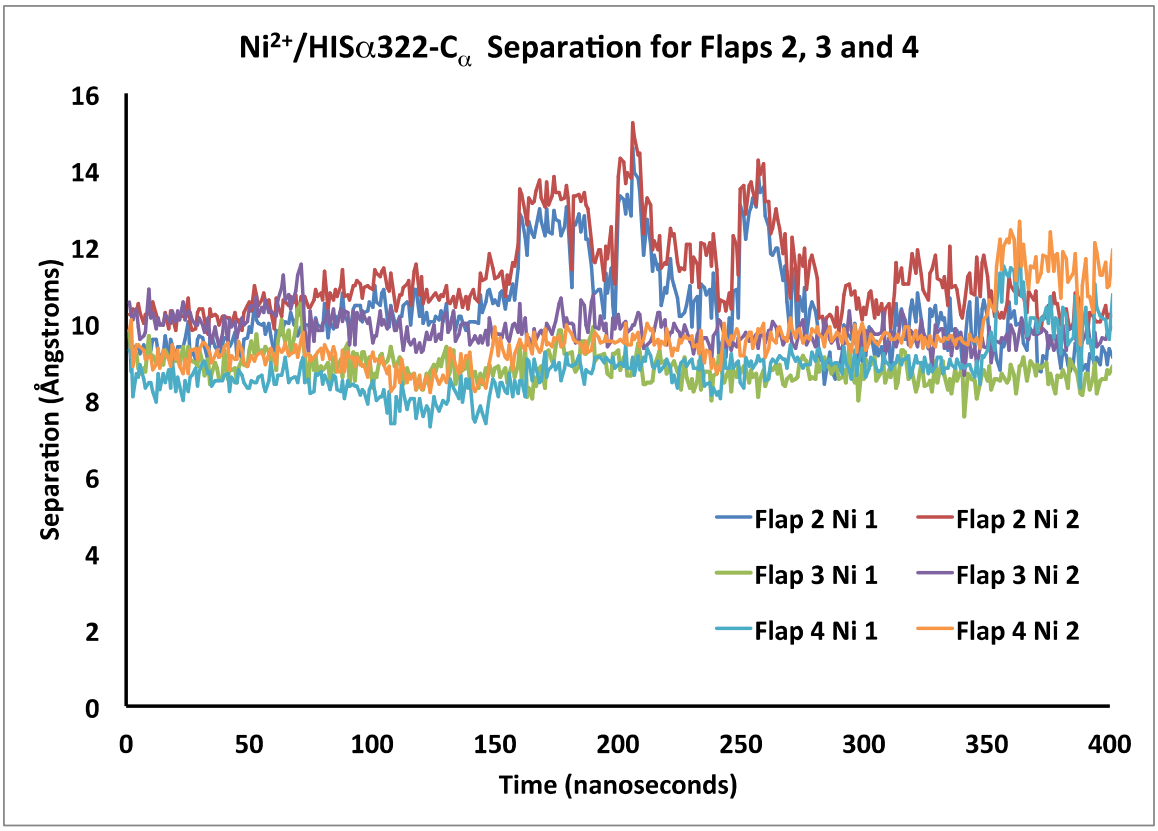

Figure S25: Flap two, three and four separations between the HISα322-C_α and each Ni^{2+} ion.

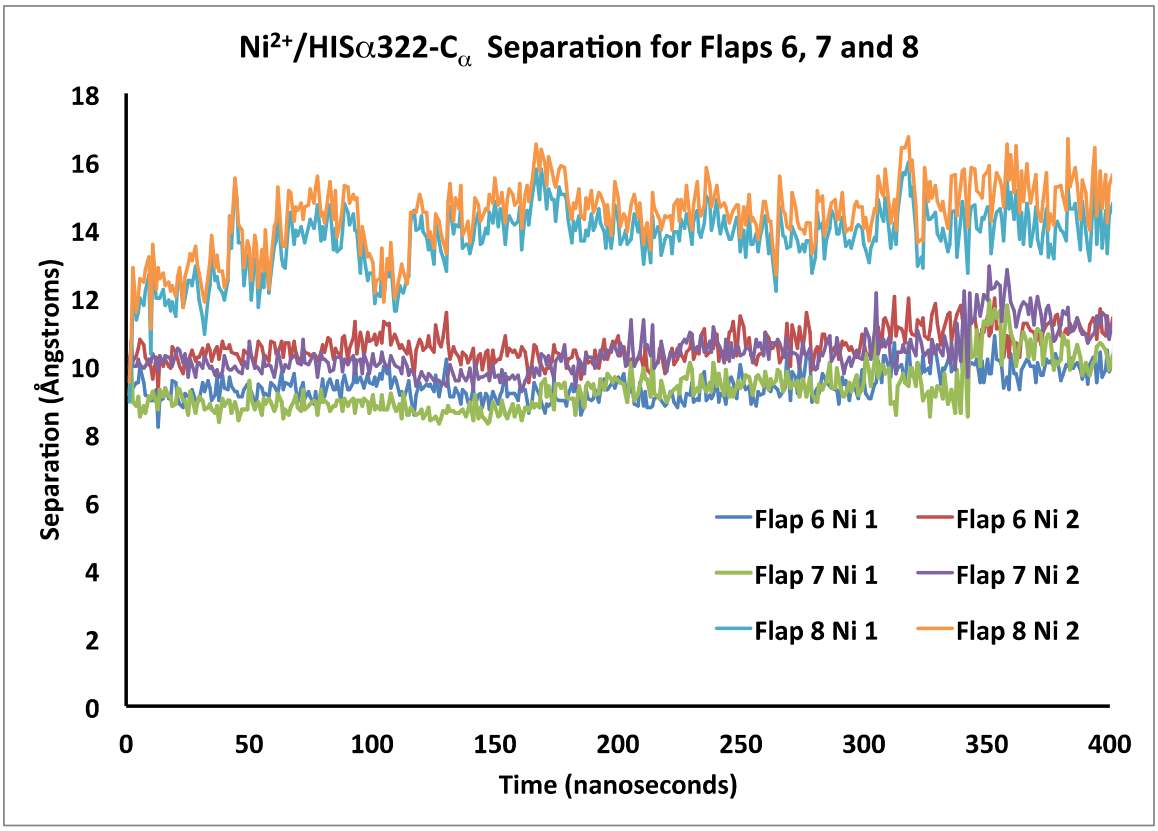

Figure S26: Flap six, seven and eight separations between the HISα322-C_α and each Ni^{2+} ion.

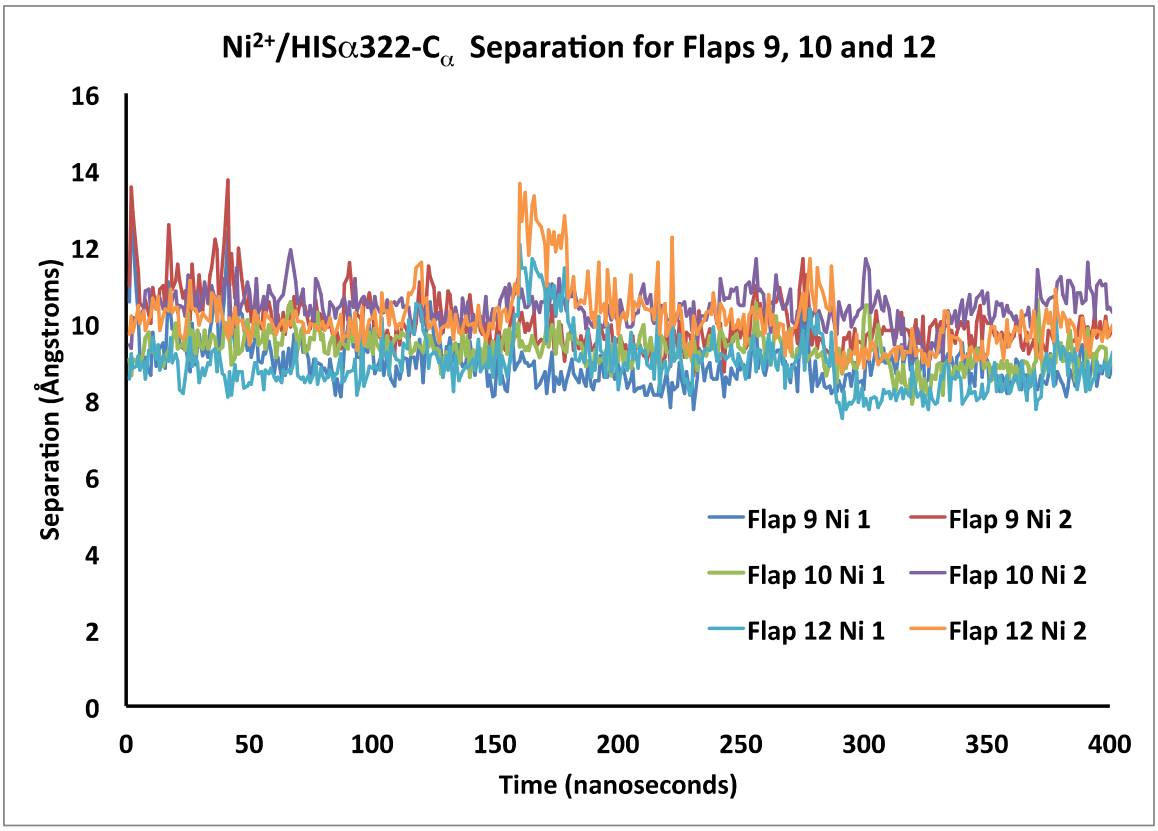

Figure S27: Flap nine, ten and twelve separations between the HISα322-C_α and each Ni^{2+} ion.

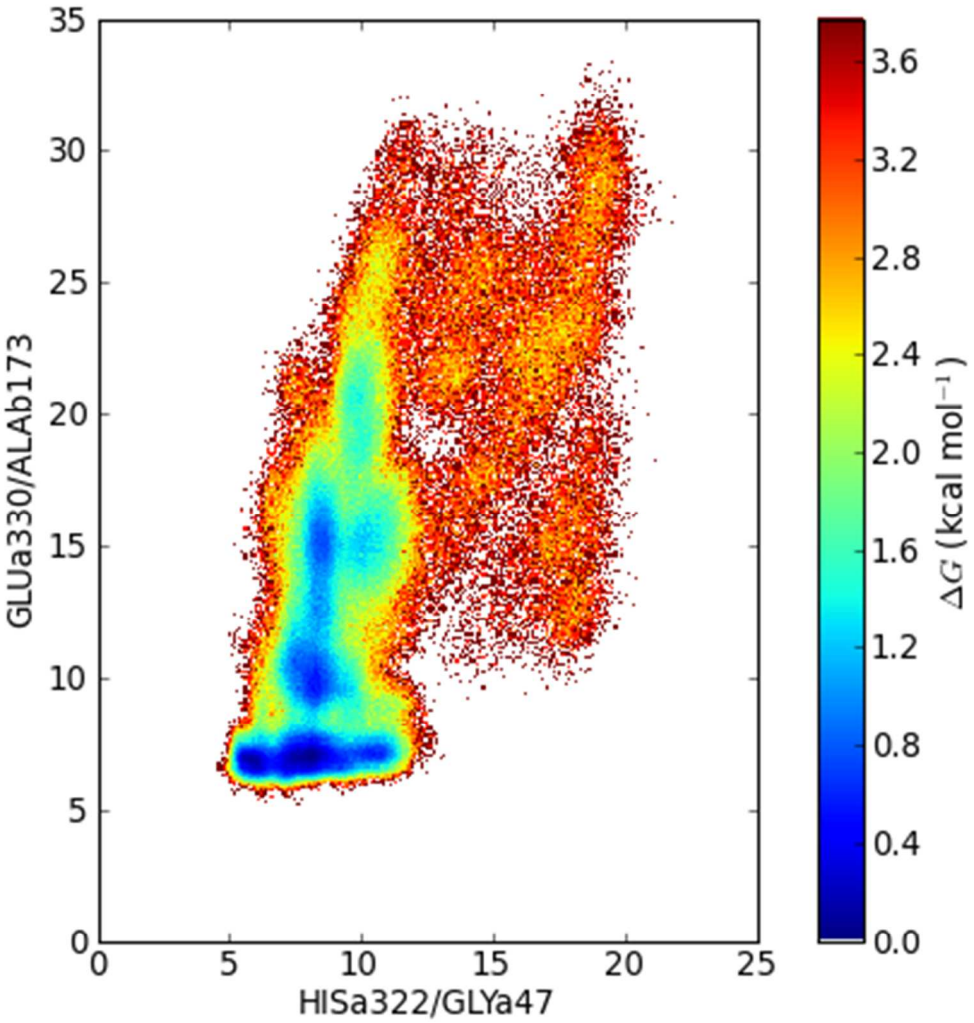

Figure S28: Relative free energy diagram constructed based on the separation between HISα322/GLYα47 (HIS/GLY) and GLUα330/ALAβ173 (GLU/ALA).

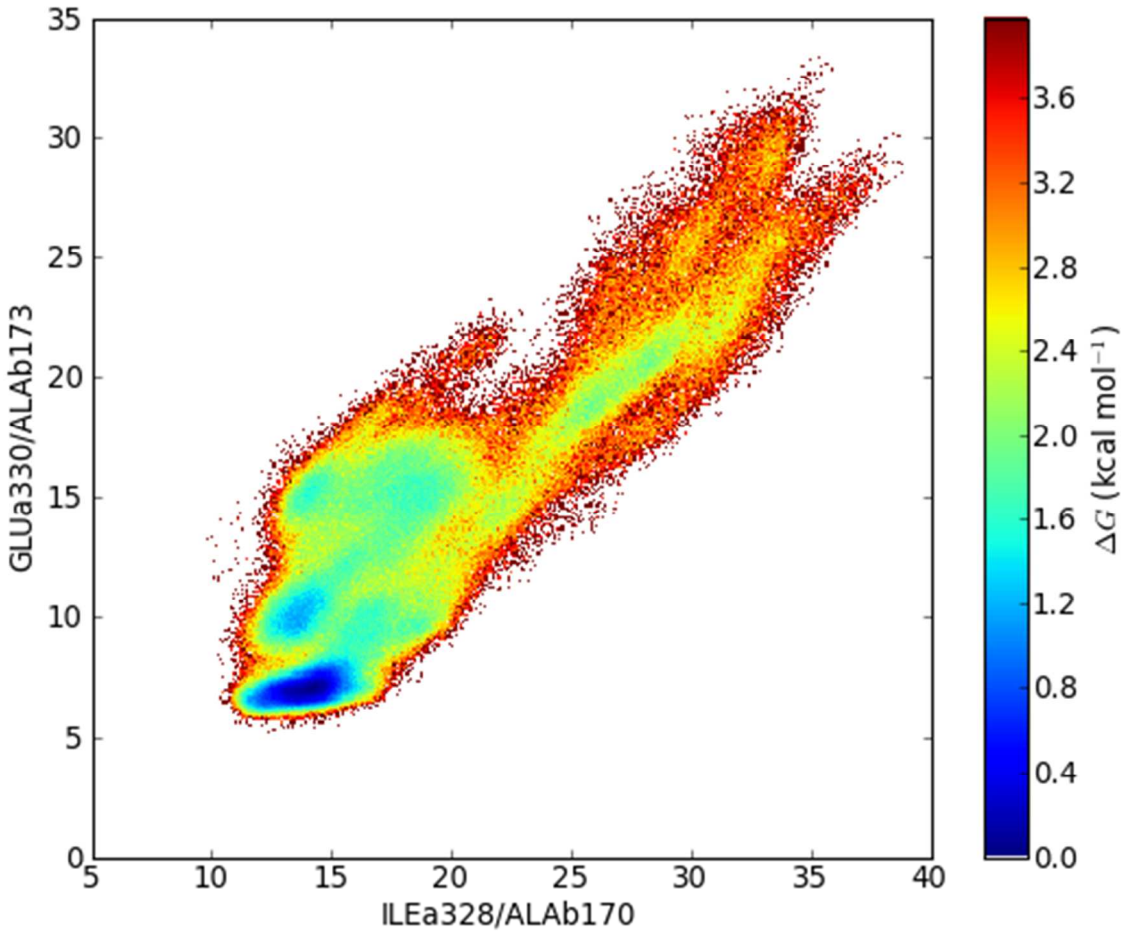

Figure S29: Relative free energy diagram constructed based on the separation between ILEα328/ALAβ170 (ILE/ALA) and GLUα330/ALAβ173 (GLU/ALA).

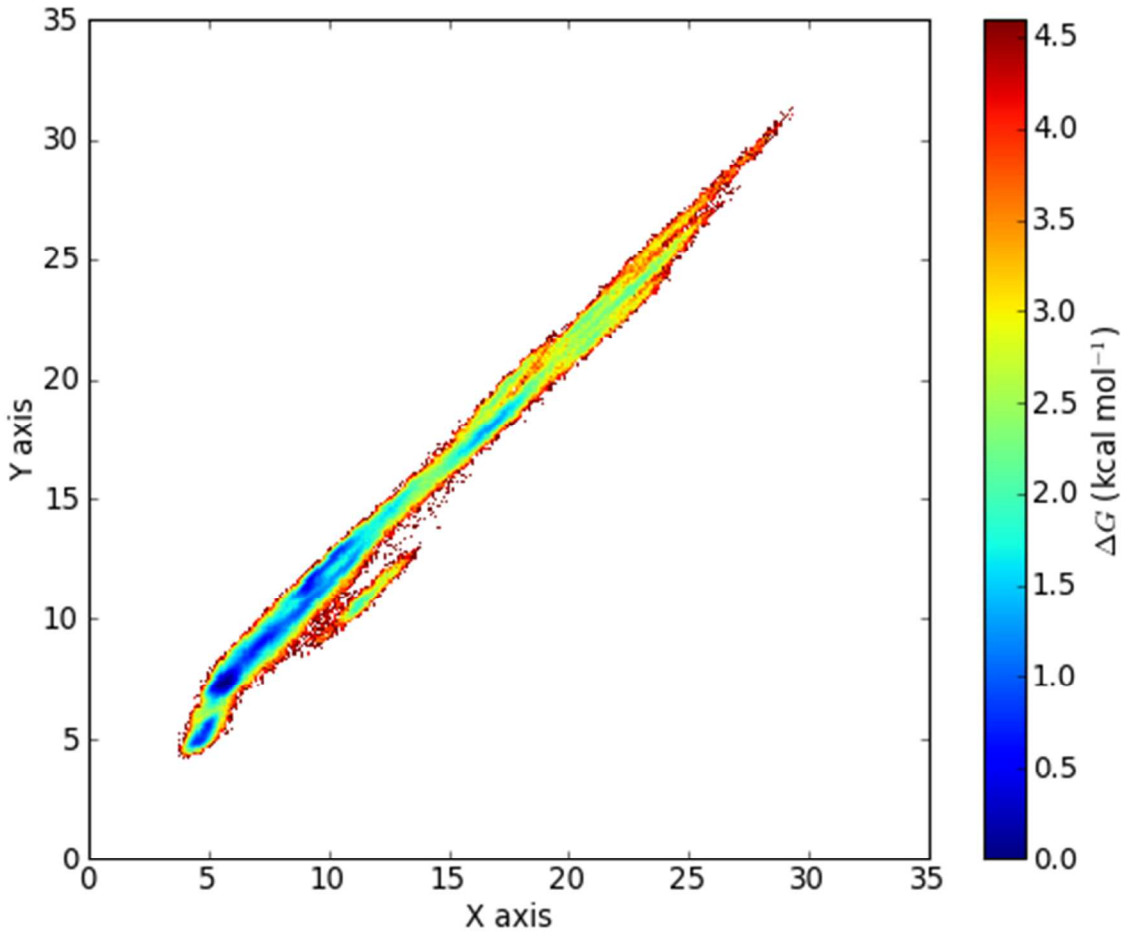

Figure S30: Relative free energy diagram HIS322εN/Ni^{2+} constructed based on the separation between (Ni1 HIS and Ni2 HIS).

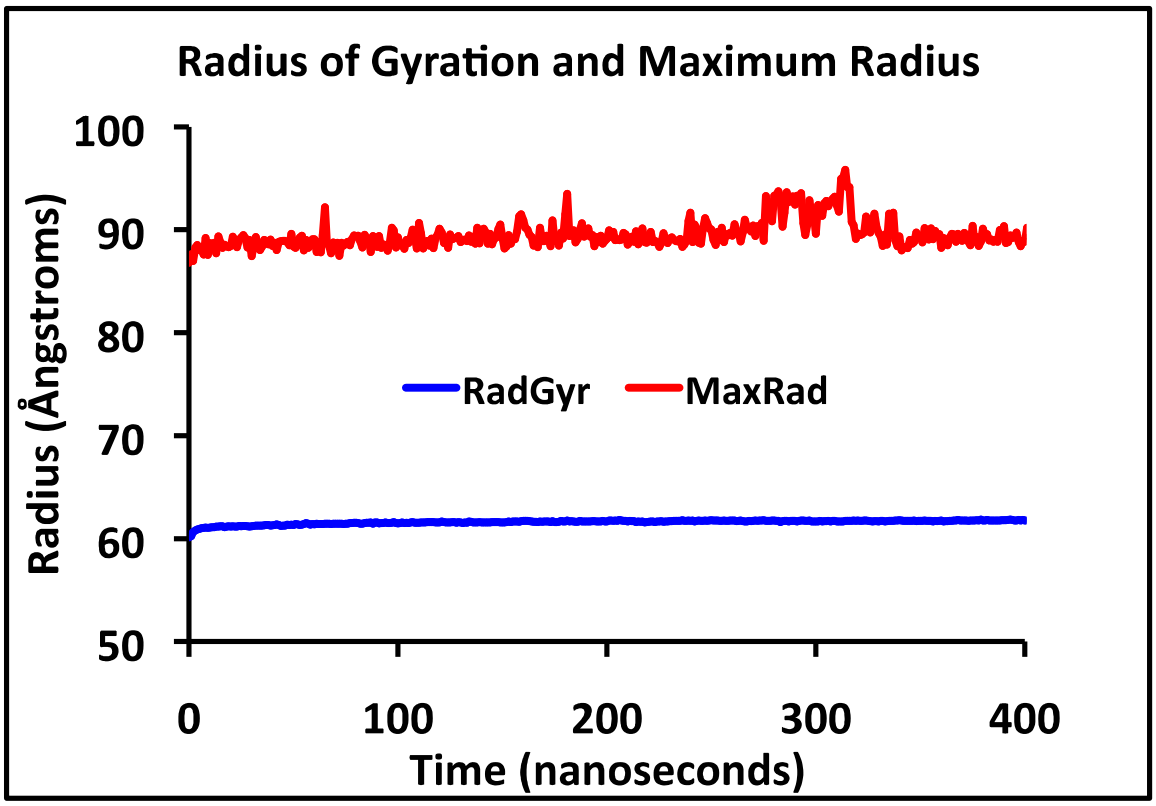

Figure S31: Radius of Gyration (blue) and Maximum Radius (red) of *H. pylori* Urease.

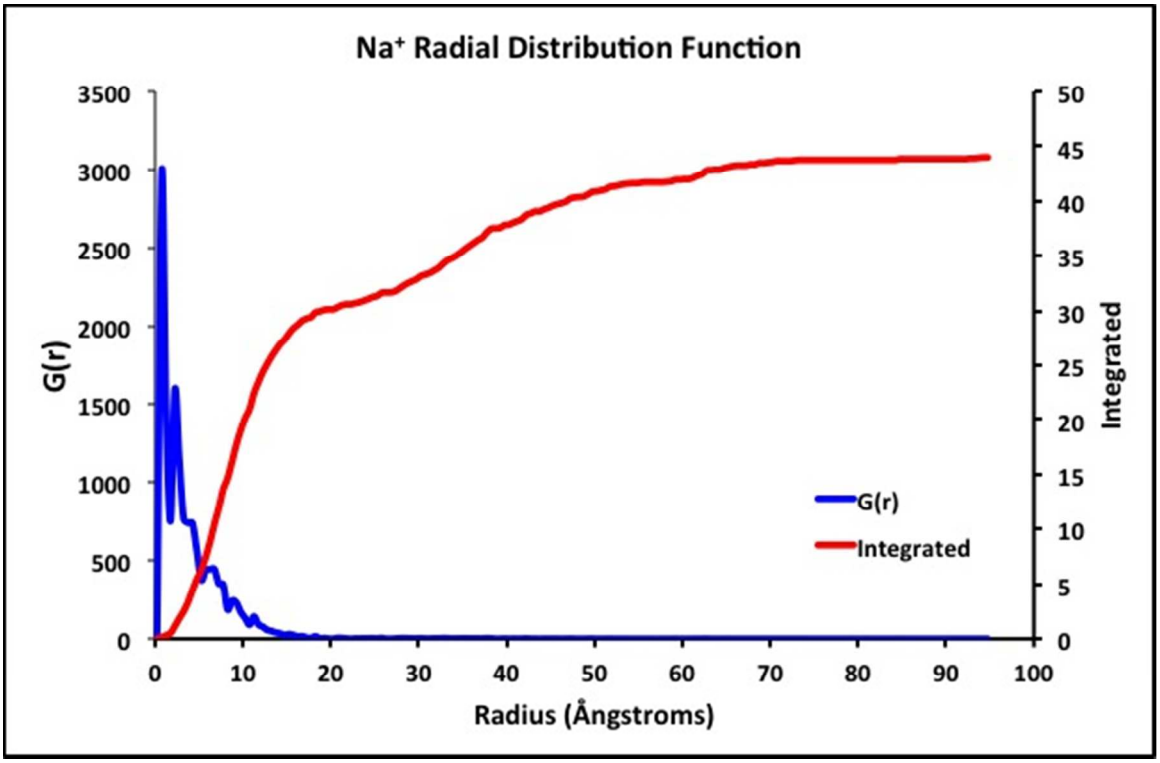

Figure S32: Na^+ Radial Distribution Function From Origin.

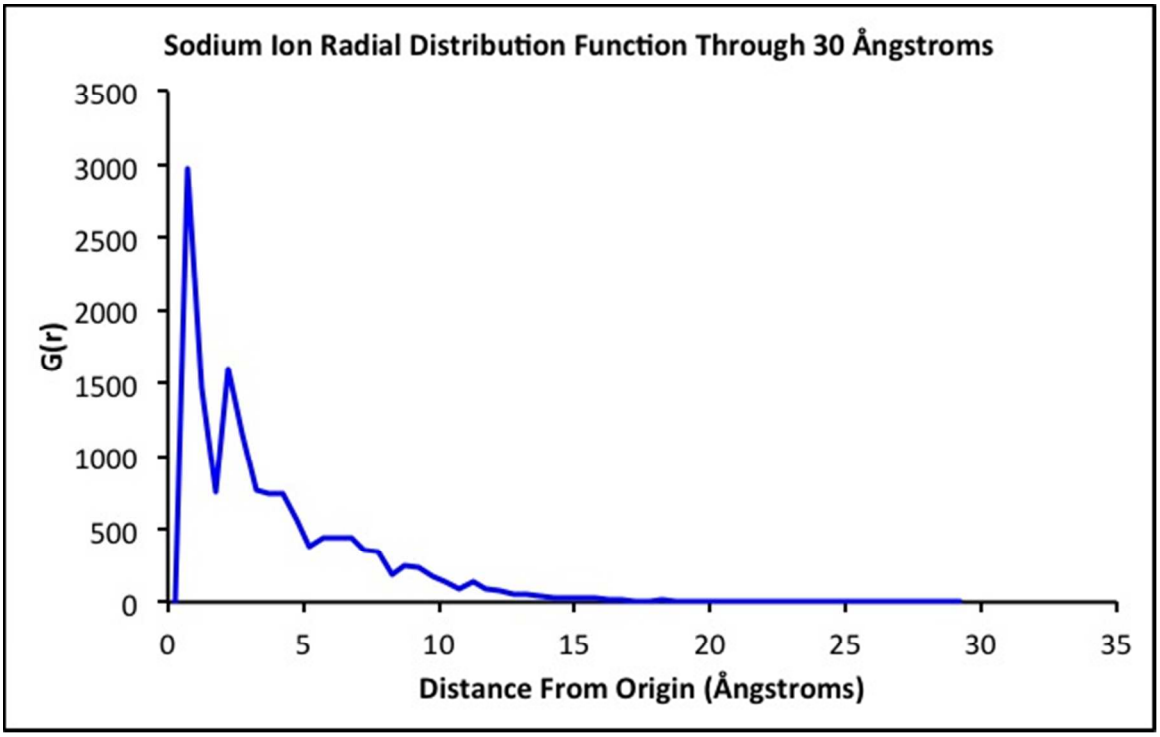

Figure S33: Na^+ Radial Distribution Function From Origin Through 30 Ångstroms.

References

(1) Karplus, P. A.; Pearson, M. A.; Hausinger, R. P. *Accounts Chem. Res.* **1997**, *30*, 330-37.

(2) Estiu, G.; Merz, K. M. *Biochemistry-Us* **2006**, *45*, 4429-43.